IEEE Access
Multidisciplinary | Rapid Review | Open Access Journal

Received June 18, 2019, accepted June 29, 2019, date of publication July 5, 2019, date of current version July 25, 2019.

Digital Object Identifier 10.1109/ACCESS.2019.2927040

Throughput Enhancement for Dual-Function Radar-Embedded Communications Using Two Generalized Sidelobe Cancellers

ABDUL RAHMAN AL-SALEHI[1], IJAZ MANSOOR QURESHI[2,3], AQDAS NAVEED MALIK[1], ZAFARULLAH KHAN[1], AND WASIM KHAN[1]

[1]Faculty of Engineering and Technology, International Islamic University, Islamabad 44000, Pakistan
[2]Department of Electrical Engineering, Air University Islamabad, Islamabad 44000, Pakistan
[3]Institute of Signals, Systems and Soft Computing (ISSS), Islamabad 44000, Pakistan

Corresponding author: Abdul Rahman Al-Salehi (alsalehi410@hotmail.com)

ABSTRACT In this paper, we develop a novel approach for a joint platform of radar and communication systems. The previous approaches for dual-function radar-communication systems focused only on the simultaneous transmission of radar and communications in radar active mode. To increase the throughput of communications without affecting the radar operation, we enable communication during the whole pulse repetition interval by using two generalized sidelobe cancellers. We propose two different operational modes of the dual-function radar-communications system. In active mode, the radar function is achieved through the mainlobe, and communications are achieved through the sidelobes. In active mode, only one generalized sidelobe canceller is functional. In rest mode, both the generalized sidelobe cancellers are functional. The first generalized sidelobe canceller has the mainlobe and sidelobe levels as in active mode, and the second generalized sidelobe canceller has the same mainlobe level but double the power in the sidelobes. The output is the difference between the two, in which the mainlobe is canceled, while the sidelobes have the same power, as in the case of active mode. The effectiveness of the proposed scheme is investigated in terms of the bit error rate. Moreover, the proposed system allows communication during the whole pulse repetition interval, thus, enhancing the throughput tremendously.

INDEX TERMS Radio spectrum management, radar signal processing, array signal processing, transmitters, wireless communication, radar antennas, multiuser detection, linear antenna arrays and multiaccess communication.

I. INTRODUCTION

The ever-increasing demands for radar and communication systems to be unified on a single platform has gained great attention from researchers in the area of spectrum sharing. This fusion is required to provide the efficient usage of the shared spectrum to obtain a high-throughput measurement of both services [1]–[4]. The most common techniques used in this technology are time sharing, frequency subbanding, and signal sharing/coding [5]. These approaches require new methods for waveform diversity manipulation with less installation, a hardware cost reduction, and radio frequency (RF) spectrum exploitation [6], [7]. Recent methods have used the same architecture and same resources for both systems to be functional simultaneously to fulfill the bandwidth demands. Such approaches can be classified as coexistence or codesign methods [8]. The coexistence approach has focused on the process of the two systems being odd functions and sources of interference to each other [9]. These systems are based on mutual information exchange and their cooperation [10]. Acodesign approach entails cooperative control inside the system to enhance the spectral efficiency of the unified platform as in [11]–[13] and the references therein. Moreover, in the explicit form of the codesign method, the information is embedded into the radar emission by varying the waveform in every radar pulse [14]–[16]. A tradeoff between the radar and communication performance by embedding information bits and keeping the waveform envelope constant with good power spectral efficiency was introduced in [15]. The concept of dual-function radar communication (DFRC) using the radar sidelobe for the communication transmission as a secondary

The associate editor coordinating the review of this manuscript and approving it for publication was Gerard-Andre Capolino.

This work is licensed under a Creative Commons Attribution 4.0 License. For more information, see http://creativecommons.org/licenses/by/4.0/

function while keeping the radar operation in the mainlobe as a primary function has been reported in many papers [6], [17]–[20]. In [17], different amplitude modulation (AM) levels and phased modulation (PM) synthesis were investigated as information-embedding-based time modulated arrays (TMAs). The radar operation takes place in the mainlobe, and information embedding takes place in the sidelobe region. The authors studied two methods. The first method was based on a sparse time modulated array (STMA), in which the antenna elements are switched on and off to produce a variation in the sidelobe level. The second method based on phase only synthesized a TMA, which is similar to an STMA, except that the variation in the sidelobe level is achieved by adjusting the phases of the transmitting array. The authors in [19] used convex optimization to allocate the radar function to the mainlobe and the secondary function of communications to the sidelobes. This method produced multiple beamforming weight vectors associated with their orthogonal waveforms having multiple sidelobe levels. Each sidelobe represents a distinct communication symbol. These sidelobe level variations or amplitude shift keying (ASK) are transmitted towards the communication receivers located in the sidelobe region of the radar. In [20], the authors used a linear combination between the principal and associated weight vectors to produce different beampatterns to be sent through the deep null towards a communication receiver. A robust technique based on quadratic and linear optimization was proposed to achieve a tradeoff between the mainlobe and sidelobes in [21]–[23]. More recent contributions to the DFRC system can be found in the literature [24]–[26]. In [24], the authors used a Butler matrix for a frequency diverse array to transmit a communication signal along the null of the radar waveform towards different ranges and directions. In [25], the authors used a time-modulated frequency diverse multiple-input and multiple-output (MIMO) array method for the DFRC system, in which the information embedding occurred via spread sequences through every radar pulse. Moreover, different radar communication integration techniques can be found in [26]. In all papers using the sidelobe approach, the obtainable communication data rate remains comparatively low, since the communication information is embedded in several waveforms only in radar active mode. Generalized sidelobe cancellers (GSCs) are an effective approach for spatial-temporal transmission. The generalized sidelobe canceller has been examined widely in radar and communication systems in areas where the desired signal needs to be measured either in time or at the amplitude level [27].

In this paper, we propose a novel approach for a dual-function radar-communications system using both radar modes to transmit communication information in a sidelobe region. The contribution of this paper can be summarized as follows:

1- We design two generalized sidelobe cancellers, GSC_1 and GSC_2. GSC_1 works in active mode to generate a radar function via the mainlobe and a communication function via the sidelobe. In rest mode, GSC_2 is functional in parallel and produces identical power in the mainlobe at the position of the mainlobe of GSC_1 but double power in the sidelobe region. Subtracting one function from the other function eliminates the mainlobe, while the sidelobes with proper power are available for the communication transmission.

2- We achieve increased throughput by using even the rest mode of the radar for communications.

The rest of this paper is organized as follows. Section II describes the fundamentals of radar, and Section III introduces the problem formulation and system modeling for the joint platform. Section IV analyzes the communication throughput per pulse repetition interval. Section V provides the simulation results. Section VI concludes the paper and discusses the future directions.

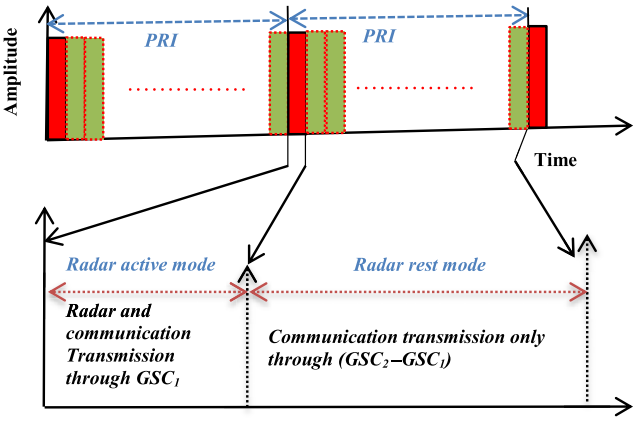

FIGURE 1. Illustrative diagram of the proposed transmission signaling of the (PRI).

II. FUNDAMENTALS

In a conventional radar system, the radar transmits energy for only a small period during each pulse repetition interval (PRI) and then remains silent with no transmission in radar rest mode, as shown in Fig. 1. Mathematically, this can be expressed as

$$T_t = t_w + \tau_r \tag{1}$$

where t_w is the radar pulse width, τ_r is the radar rest mode time for the transmitted pulse reflection from the target during one PRI, and T_t is the total time for one pulse repetition interval. To calculate the time taken by the target echo, one should know the distance of the target and the time associated with the pulse width during each PRI. In doing so, two parameters need to be considered. The first parameter involves the relation between the active mode and rest mode time duration during each PRI according to the following equation:

$$\tau_r = T_t - t_w \tag{2}$$

The second parameter is the rest mode time based on the target distance. The target distance corresponds to the two-way propagation time of the transmitted pulse during each

PRI from the radar transmitter to the target, which is backscattered and received before the next pulse is transmitted. This relation is given as

$$\mathcal{R}_{\max} = \frac{(t_w + \tau_r)C}{2} \tag{3}$$

where C is the speed of light and $\mathcal{R}_{\max}$ is the maximum unambiguous range. Hence, the maximum time given for rest mode based on the maximum unambiguous range can be given as

$$\tau_r = \frac{2\mathcal{R}_{\max}}{C} - t_w \tag{4}$$

III. PROBLEM FORMULATION AND SYSTEM MODEL

The communication data rate for information embedding based on the sidelobe remains unchanged and bounded only by the sidelobe occurrence in radar active mode. To increase the communication throughput, we propose a technique that allows communication transmission during the radar active and rest modes. In active mode, GSC_1 works and tracks the signal for the radar via the mainlobe and communication signal via the sidelobe.

The processing time in active mode is t_w. In rest mode, GSC_1 and GSC_2 work together; having identical amplitude powers in the mainlobe and different amplitude powers in the sidelobe region. The subtracted resulting power of both GSCs (GSC_1 and GSC_2) is transmitted during the time τ_r.

In this paper, we consider a uniform linear array of M transmit antenna elements with a spacing of d. These elements simultaneously transmit the radar waveform and communication signal in radar active mode, while they carry out only the communication process in radar rest mode, i.e., with no radar transmission. It is worth mentioning that we consider the case of a single target in this paper.

A. DFRC IN RADAR ACTIVE MODE

The optimization problem for the simultaneous transmission of the desired radar waveform through the mainlobe (as a primary function) and the communication waveform through the sidelobe region (as a secondary function) is given by the following expressions:

$$\min_{\mathbf{w}_1} \max_{\theta} \left| \mathbf{w}_1^H \mathbf{a_1}(\theta) \right| \tag{5a}$$

$$\text{s.t } \mathbf{w}_1^H \mathbf{a_1}(\theta_t) = 1, \quad \theta_t \in \tag{5b}$$

$$\mathbf{w}_1^H \mathbf{a}(\theta_{ci}) = \Delta_{1,i} e^{\Omega_i} \quad \text{for } 1 \le i \le k-1 \tag{5c}$$

In the above expressions, $\mathbf{w}_1$ is an M-by-1 weight vector, $(.)^H$ is a Hermitian operator, $\mathbf{a_1}(\theta_t)$ is an M-by-1 steering vector towards the target at θ_t in radar spatial sector Θ, $\mathbf{a_1}(\theta_{ci})$ is an M-by-1 steering vector towards a predefined i^{th} communication receiver located at angle (θ_{ci}) and $\Delta_{1,i}e^{\Omega_i}$ is the desired communication signal strength in the relevant sidelobe region.

To implement this optimization problem, we use a generalized sidelobe canceller (GSC_1) as shown in Fig. 2 for the transmission in radar active mode. The parameters for the proposed GSC_1 are given as follows:

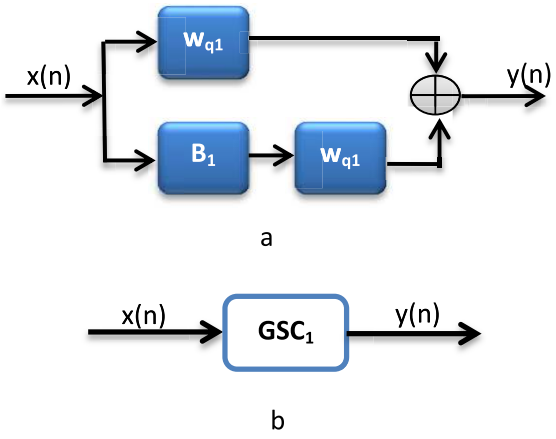

FIGURE 2. (a) Block diagram of the generalized sidelobe canceller (GSC). (b) Is equivalent to (a).

The constraint matrix is:

$$\mathbf{C_1} = \left[\bar{a}(\theta_t) \quad \bar{a}(\theta_{c1}) \quad \bar{a}(\theta_{c2}) \ldots \quad \bar{a}(\theta_{k-1}) \right] \tag{6}$$

The blocking matrix is:

$$\boldsymbol{B_1} = \text{null}\left[\mathbf{C_1^H}\right] \tag{7}$$

The gain vector is:

$$\mathbf{C_1^H w_1} = \mathbf{f_1} \tag{8}$$

The quiescent weight vector is:

$$\mathbf{w}_{q1} = \mathbf{C_1}(\mathbf{C_1^H C_1})^{-1} \boldsymbol{f_1} \tag{9}$$

The adjustable weight vector is:

$$\mathbf{w_{a1}} = (\mathbf{B_1^H} \boldsymbol{R_x} \mathbf{B_1})^{-1} \mathbf{B_1 R w}_{q1} \tag{10}$$

where k denotes the number of columns in $\mathbf{C_1}$, $k-1$ represents the number of communication directions, and $\mathbf{C_1}$ is the M-by-k constraint matrix of the total steering vectors. $\boldsymbol{B_1}$ is the M-by-(M-k) blocking matrix of the space spanned by the columns of the steering vector contained in the matrix, and $(.)^{-1}$ is the inverse operator. $\mathbf{f_1}$ is the gain vector for k constraints (in our scenario, k = 5), and $\boldsymbol{R_x}$ is the correlation matrix. The transmitted steering vector towards the direction i can be expressed in general form as

$$\bar{a}(\theta_i) = [1 \; e^{-j\left(\frac{2\pi \sin\theta_i}{c}\right)}, \ldots\ldots\ldots e^{-j\left(\frac{2\pi (M-1)\sin\theta_i}{c}\right)}]^T \tag{11}$$

where $[.]^T$ is the transpose operator. For our approach, the optimum weight vector that minimizes the mean square value of the beamformer output is subject to multiple linear constraints and may be expressed as

$$\mathbf{f_1} = \mathbf{C^H w_1} = \begin{bmatrix} \chi \\ \Delta_{1,1}e^{\Omega_1} \\ \Delta_{1,2}e^{\Omega_2} \\ \Delta_{1,3}e^{\Omega_3} \\ \Delta_{1,4}e^{\Omega_4} \end{bmatrix} \tag{12}$$

where

$$e^{\Omega_i} = \begin{cases} e^{\mathbf{0}}, & for\ \Omega = 0 \\ e^{\mathbf{1}}, & for\ \Omega = 1 \end{cases} \tag{13}$$

Here, $\chi = 1$ represents the unit value gain along θ_t for the radar signal power towards the target. $\Delta_{1,i}e^{\Omega_i}$ is the desired communication signal, where the values of Δ in column represent the communication power in the sidelobe region and $\Omega \in [0, 1]$ represents binary information bits associated with each sidelobe level. If the received beampattern has a higher sidelobe level, then the transmitted bit is one; otherwise, it is zero.

To find the blocking matrix, as given in [28], the orthogonal complement is written as

$$\mathbf{C}_1^H \boldsymbol{B}_1 = 0 \tag{14}$$

where 0 denotes the null matrix. Thus, the gain vector may be rewritten as

$$\mathbf{C}^{\mathrm{H}}\left(\mathbf{w}_{\mathrm{q1}}\right) = \begin{bmatrix} \chi \\ \Delta_{1,1}e^{\Omega_1} \\ \Delta_{1,2}e^{\Omega_2} \\ \Delta_{1,3}e^{\Omega_3} \\ \Delta_{1,4}e^{\Omega_4} \end{bmatrix} \tag{15}$$

where $\mathbf{w_{q1}}$ is the quiescent beamformer that guarantees the communication signal in the desired direction. $\mathbf{w_{q1}}$ is fixed and is not affected by the lower branch of GSC_1. For an unconstrained optimization problem, we should only adjust the weight vector available in the lower branch i.e., $\mathbf{w}_{\mathrm{a1}}$. If we consider the output signal of the first GSC_1 given as

$$\mathbf{W}_{\mathrm{q1}}^{\mathrm{H}}\mathbf{x}(\mathrm{n}) - \mathbf{w}_{\mathbf{a1}}^{\mathbf{H}}\mathbf{B}_{\mathbf{1}}^{\mathbf{H}}\mathbf{x}(\mathrm{n}) = y_1(n) \tag{16}$$

then its corresponding output power is written as

$$\begin{aligned} \mathrm{E}\left|y_1(n)\right|^2 &= \left(\mathbf{w}_{\mathrm{q1}} - \mathbf{B}_1\mathbf{w}_{\mathrm{a1}}\right)^H \boldsymbol{E}\left[\mathbf{x}^*(\mathrm{n})\mathbf{x}(\mathrm{n})\right]\left(\mathbf{w}_{\mathrm{q1}} - \mathbf{B}_1\mathbf{w}_{\mathrm{a1}}\right) \\ \mathrm{E}\left|y_1(n)\right|^2 &= \left(\mathbf{w}_{\mathrm{q1}} - \mathbf{B}_1\mathbf{w}_{\mathrm{a1}}\right)^H \boldsymbol{R_x}\left(\mathbf{w}_{\mathrm{q1}} - \mathbf{B}_1\mathbf{w}_{\mathrm{a1}}\right) \\ &= P_{GSC_1} \end{aligned} \tag{17}$$

Here, the correlation matrix $\boldsymbol{R_x}$ of the five constraints can be expressed as

$$\boldsymbol{R_x} = \boldsymbol{R_t} + \boldsymbol{R_{c1}} + \boldsymbol{R_{c2}} + \boldsymbol{R_{c3}} + \boldsymbol{R_{c4}} \tag{18}$$

where $\boldsymbol{R_t}$ is the radar correlation matrix and $(\boldsymbol{R_{c1}} + \boldsymbol{R_{c2}} + \boldsymbol{R_{c3}} + \boldsymbol{R_{c4}})$ are the communication correlation matrices. The correlation matrix of these signals is given as

$$\boldsymbol{R_x} = \begin{bmatrix} \boldsymbol{\sigma}_1^2 & \cdots & \mathbf{0} \\ \vdots & \boldsymbol{\sigma}_2^2 & \vdots \\ \mathbf{0} & \cdots & \boldsymbol{\sigma}_i^2 \end{bmatrix} \tag{19}$$

$\left\{\boldsymbol{\sigma}_i^2\right\}_i^M$ is the power of each transmitted signal. $\boldsymbol{R_x} = \boldsymbol{\sigma}^2\mathbf{I}$ in the case of white noise only, where $\mathbf{I}$ is the M-by-M identity matrix and $\boldsymbol{\sigma}^2$ is the noise variance. Thus, Eq. (10) may be rewritten as

$$\mathbf{w_{a1}} = \left(\mathbf{B}_{\mathbf{1}}^{\mathbf{H}}\mathbf{B_1}\right)^{-1}\mathbf{B_1}\mathbf{w}_{\mathbf{q}_1} \tag{20}$$

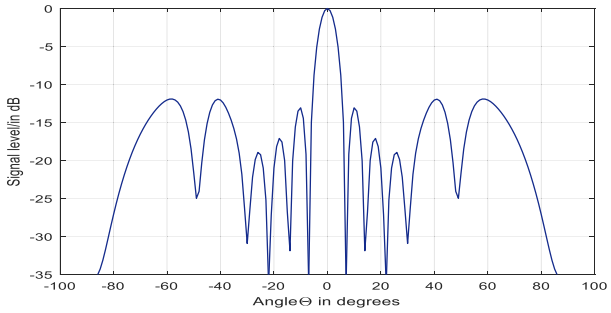

FIGURE 3. Beampattern during GSC_1 to transmit a radar signal towards the target and four communication signals.

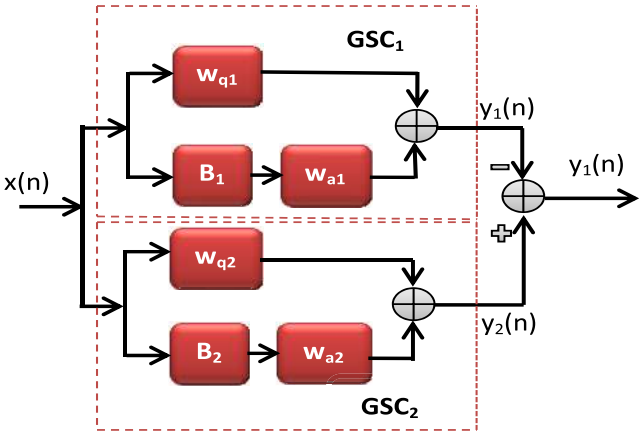

FIGURE 4. Proposed technique for the joint transmitter system.

B. TRANSMISSION IN RADAR REST MODE

In this mode, no signal should be transmitted in the direction of the target, while the communication waveforms should continue through the prescribed sidelobe regions. For this purpose, GSC_2 starts functioning in parallel to GSC_1. To cancel the signal in the direction of the target, the signal strengths of both GSCs in the mainlobe are kept identical. Ideally, the subtraction of the signals of these GSCs shown in Fig. 4 will result in no signal in the mainlobe region. On the other hand, the signal strength of GSC_2 in the prescribed sidelobe regions is kept double that of GSC_1. Therefore, the overall signal strength after the subtraction will be the same as in radar active mode for the sidelobe communication. To formulate this problem, we design a weight vector $\mathbf{w}_2$ that adjusts the GSC_2 radiation power to be identical to that of GSC_1 except that the sidelobe power of GSC_2 is double that of GSC_1. Such a weight vector can be formulated by the following optimization problem:

$$\min_{\mathbf{w}_2} \max_{\theta} \left|\mathbf{w}_2^{\mathrm{H}}\mathbf{a}_2(\theta)\right| \tag{21a}$$

$$\text{s.t } \mathbf{w}_2^{\mathrm{H}}\mathbf{a}_2\left(\theta_{\mathrm{t}}\right) = 1, \quad \theta_{\mathrm{t}} \in \Theta \tag{21b}$$

$$\mathbf{w}_2^{\mathrm{H}}\mathbf{a}_2\left(\theta_{\mathrm{ci}}\right) = \Delta_{2,i}e^{\Omega_i} \quad \text{for } 1 \le i \le 4 \tag{21c}$$

where $\mathbf{w}_2$ is the M-by-1 weight vector of GSC_2. In our case, both *GSCs* have overlapping main beams and communication sidelobes. Thus, $\mathbf{C}_1 = \mathbf{C}_2$ and $\mathbf{B}_1 = \mathbf{B}_2$. The blocking matrix

of the space spanned by the columns of the steering vector matrix $\mathbf{C}$ of GSC_2 is identical to that in GSC_1; therefore, the GSC_2 parameters can be written as follows.

The constraint matrix is:

$$\mathbf{C}_2 = [\overline{a}(\theta_t) \quad \overline{a}(\theta_{c1}) \quad \overline{a}(\theta_{c2}) \ldots \quad \overline{a}(\theta_{k-1})] \tag{22}$$

The blocking matrix is:

$$\boldsymbol{B}_2 = \text{null}\left[\mathbf{c}_2^{\text{H}}\right] \tag{23}$$

The gain vector is:

$$\mathbf{C}_2^{\mathbf{H}}\mathbf{w}_2 = \mathbf{f}_2 \tag{24}$$

The quiescent weight vector is:

$$\mathbf{w}_{q2} = \mathbf{C}_2\left(\mathbf{C}_2^{\text{H}}\mathbf{C}_2\right)^{-1}\boldsymbol{f}_2 \tag{25}$$

The adjustable weight vector is:

$$\mathbf{W}_{a2} = \left(\mathbf{B}_2^{\boldsymbol{H}}\boldsymbol{R}_{\boldsymbol{x}}\mathbf{B}_2\right)^{-1}\mathbf{B}_2\boldsymbol{R}_{\boldsymbol{x}}\mathbf{W}_{\mathbf{q2}} \tag{26}$$

$$\mathbf{w}_{a1} = \left(\mathbf{B}_2^{\mathbf{H}}\mathbf{B}_2\right)^{-1}\mathbf{B}_2\mathbf{w}_{q2} \tag{27}$$

The gain vector $\mathbf{f}_2$ for the multiple linear constraints of the second *GSC* may be expressed as

$$\mathbf{C}_2^{\mathbf{H}}\mathbf{w}_2 = \mathbf{f}_2 = \begin{bmatrix} \chi \\ 2\Delta_{2,1}e^{\Omega_1} \\ 2\Delta_{2,1}e^{\Omega_2} \\ 2\Delta_{2,3}e^{\Omega_3} \\ 2\Delta_{2,4}e^{\Omega_4} \end{bmatrix} \tag{28}$$

Similar to the previous gain vector in GSC_1, in which the first value in the column represents the normalized radar power towards the target and the rest of the values are the communication powers in the sidelobe region. The values of this communication gain vector are double those in the first gain vector $\mathbf{f_1}$.

For an unconstrained optimization problem, one should adjust the lower branch, the weight vector $\mathbf{w}_{a2}$. The signal power of the second GSC_2 can be written as

$$\mathbf{w}_{\mathbf{q2}}^{\mathbf{H}}\mathbf{x}(\mathrm{n}) - \mathbf{w}_{\mathbf{a2}}^{\mathbf{H}}\mathbf{B}_2^{\mathbf{H}}\mathbf{x}(\mathrm{n}) = y_2(n) \tag{29}$$

By taking the expected value of the above equation, its corresponding output power is written as

$$\begin{aligned} \mathrm{E}\,|y_2(n)|^2 &= \left(\mathbf{w}_{q2} - \mathbf{B}_2\mathbf{w}_{a2}\right)^{\boldsymbol{H}}\boldsymbol{E}\left[\mathbf{x}^*(\mathrm{n})\mathbf{x}(\mathrm{n})\right]\left(\mathbf{w}_{q2} - \mathbf{B}_2\mathbf{w}_{a2}\right) \\ \mathrm{E}\,|y_2(n)|^2 &= \left(\mathbf{w}_{q2} - \mathbf{B}_1\mathbf{w}_{a2}\right)^{\boldsymbol{H}}\boldsymbol{R}_{\boldsymbol{x}}\left(\mathbf{w}_{q2} - \mathbf{B}_1\mathbf{w}_{a2}\right) \\ &= P_{GSC_2} \end{aligned} \tag{30}$$

It is worth mentioning that we have assumed the same power in the mainlobes for both GSCs, but GSC_2 has double the power in the sidelobe region compared to GSC_1. Hence, the resultant power of both GSCs can be written as

$$\mathrm{E}\,|y_2(n)|^2 - \mathrm{E}\,|y_1(n)|^2 = \Delta \tag{31}$$

This Δ represents the net power in the sidelobe region, i.e., with no power in the mainlobes in radar rest mode, as shown in Fig. (5). Note that this power in the sidelobe region is equal to the power in the sidelobe region of GSC_1. Moreover, a comparison of the proposed technique with the existing DFRC methods in terms of radar operating modes is shown in Table 1.

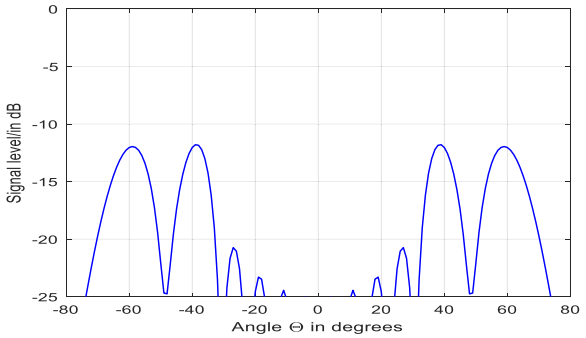

FIGURE 5. Beampattern in radar rest mode.

TABLE 1. Radar operating modes for different DFRC systems.

Radar Mode	In Active Mode		In Rest Mode	
Transmission type	Radar Tx	Comm. Tx	Radar Tx	Comm. Tx
All existing DFRC transmissions	On: in mainlobe	On: in sidelobe	Off	Off
PE-MU-DFRC[29]	On: in mainlobe	On: in sidelobe	Off	Off
Proposed technique: GSC-DFRC	On: in mainlobe	On: in sidelobe	Off	On: in sidelobe

IV. COMMUNICATION THROUGHPUT PER PRI

We consider a radar operating in active mode for tracking purposes. In our scenario, the radar and communications have the same waveform. During one PRI, the communication transmission has two achievable rates: one rate in active mode denoted by $\mathrm{q_w}$ and another rate in rest mode represented by $\mathrm{q_r}$, where $\mathrm{q_w} \leq q_r$. The ratio of the transmitted communication to the pulse repetition interval is known as the throughput Q. The throughput in active mode can be formulated as

$$Q_w = \frac{\mathrm{t_w}}{\mathrm{T_t}} \tag{32}$$

where $\mathrm{T_t}$ is the total time of one pulse repetition interval. In the literature, the throughput for communication has been taken in active mode only. To increase the communication throughput, we propose a technique that transmits the communication and inhibits the radar transmission during the radar rest mode duration τ_r. The increase in the throughput in radar rest mode for the communication can be written as

$$\mathrm{Q}_{increased} = \frac{\tau_\mathrm{r}}{\mathrm{T_t}} \tag{33}$$

The total throughput for a communication link during one pulse repetition interval is

$$\mathrm{Q}_{max} = \mathrm{Q}_w + \mathrm{Q}_{increased} = \frac{\mathrm{t_w}}{\mathrm{T_t}} + \frac{\tau_\mathrm{r}}{\mathrm{T_t}} \tag{34}$$

TABLE 2. A comparative summary of the data rates achieved for the previous existing techniques.

Signaling strategy	*Domain*	*Parameters Exploited*	*Existing maximum data rate= $Q_w = Q_{during\ active\ mode}$*	*Proposed maximum data rate= Q_{max} (Eq. (34); if applied to any existing DFRC)*
Sidelobe AM [17]	*Spatial*	*W= L ≥2 , R=1,B=1 per pulse , K=1*	$Q_w = log_2 L$	$Q_w + Q_{increased} = (log_2 L)_w + (log_2 L)_{increased}$
Sidelobe-based multiwaveform ASK [19]	*Spatial*	*(W_l=W_{low} for B=1, W_2=W_{high} for B=0) during each K. K(≤ k) is fixed, where k is the possible K to be transmitted.*	$Q_w = K\ log_2 L$	$Q_w + Q_{increased} = (K\ log_2 L)_w + (K\ log_2 L)_{increased}$
Multiwaveform single-level ASK [30]	*Spatial*	*W_l=W_{high} is related to the highest L. (K and R vary).* For all zeros, *K*=1. $B_{l,k}$=1 else: $B_{l,l}$=0, $B_{1,k}$=0 or 1,$\sum_{k=1}^{K} B_{1,k} = K$	Q_w=K≤k, *where k is the possible K reached for R.*	$Q_w + Q_{increased} = (K \leq k)_w + (K \leq k)_{increased}$
Multiuser ASK [18]	*Spatial*	*$W = L^R$ and L vary for distinct SLL. K and B vary.*	$Q_w = RK\ log_2 L$	$Q_w + Q_{increased} = (RK log_2 L)_w + (RK log_2 L)_{increased}$
Sidelobe-based QAM, Ref. (31)	*Spatial*	*$W = (LP)^R$, L ,P,R, and K vary.*	$Q_w = RK\ log_2 LP$	$Q_w + Q_{increased} = (RK log_2 LP)_w + (RK log_2 LP)_{increased}$
Sidelobe-based GSC (proposed)	*Spatiotemporal*	*Two weight vectors are transmitted during different radar modes to multiple communication receivers. W=2, K=2, R=4,(B=1 or 0; Eq.(13)).*	$Q_w + Q_{increased} = (RK\ log_2 L)_w + (RK\ log_2 L)_{increased}$	

The increase in the throughput is given as

$$(Q_{max}/Q_w) = \frac{t_w + \tau_r}{t_w} = 1 + \tau_r/t_w \tag{35}$$

In addition, we assume L sidelobe levels transmitting information to *R* receivers located in the sidelobe region. According to our optimization problem, log_2L bits of information can be transmitted to each communication receiver. The maximum number of bits transmitted during each pulse repetition interval can be written (RKlog_2L in active mode + RK log_2L in radar rest mode), where K is the radar waveform. In contrast, for the same setup, the authors in [18] transmitted only RKlog_2L in active mode. The difference between our proposed scheme and all existing methods is that the proposed technique has a higher throughput because the communication transmission is conducted during both modes of the radar, the active and rest modes. Furthermore, for the same transmitted beam, each sidelobe has its own distinct power level. To validate this claim, we investigate the transmission of the same beampattern towards different sidelobe directions with different power levels, as shown in the simulation section. Table 2 shows a comparative summary of the data rates achieved for the previous existing techniques and the corresponding enhancement proposed in this paper with the (*GSC-DFRC*) method. The abbreviations in this table are as follows: *W* is the weight vector, *L* is the number of sidelobe levels, *B* is the bits per pulse, *K* is the radar waveform, *R* is the communication constraints towards each communication receiver, and *P* is the distinct phase of every communication receiver. These parameters are used in the literature for problem optimizations such as in Eq. (5).

V. SIMULATION RESULTS

In our simulation, we consider a uniform linear array with 16 transmitting antenna elements with an interelement spacing of *d* and half a wavelength. We proved that the radar function during its active mode is not influenced by the communication transmission in the sidelobe region. The throughput as a function of time was also calculated. The following examples explain the simulation results.

Example 1 (GSCs Behavior During the PRI):

In this example, we validate the idea of using two GSCs. Fig. (6) shows that GSC_1 functions in active mode operation and is represented by a red line. The GSC_1 radiation pattern includes a radar signal towards the target and four communication signals with the same waveform towards their intended communication receivers. The radiation pattern transmits a radar signal for tracking purposes via the mainlobe towards $\theta_t = 0°$ and a communication signal in the sidelobe region towards $\theta_{c1} = -60°$, $\theta_{c2} = -40°$, $\theta_{c3} = 40°$ and $\theta_{c4} = 60°$. The resulting subtraction of both GSCs is represented by the blue dashed line and functions in rest mode. The communication transmission that occurs in the sidelobe in active mode keeps the radiation towards their receivers in rest mode. The communication signal in rest mode is identical to the communication signal that occurs in the sidelobe in radar active mode. It is assumed that both radiation patterns have the same null position for both GSCs for the main and sidelobe regions. The sidelobe levels of both beams have equal power levels.

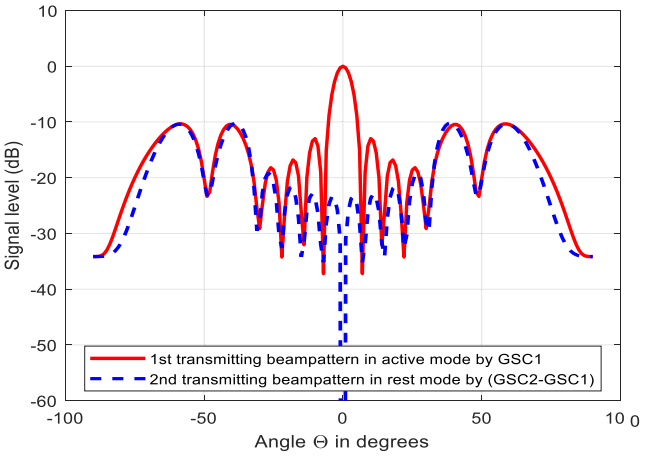

FIGURE 6. First beampattern through GSC_1 in radar active mode (red line) and the second beampattern through (GSC_2-GSC_1) in radar rest mode (blue dashed line) (Example 1).

Example 2 (DFRC Transmission in Active Mode):

During the active radar mode time, we design two beampatterns with the same power in the mainlobe towards a radar target, and in the same time, we allow variable sidelobe levels of the two beampatterns to represent the communication information transmitted towards the four communication directions. In Fig.7(a), the communication sidelobe

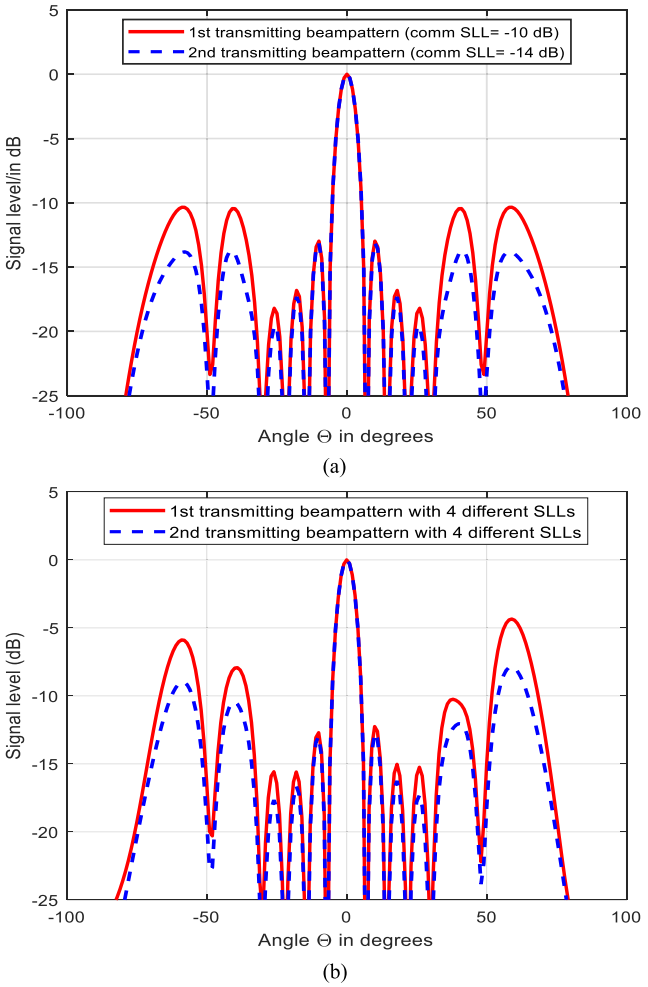

FIGURE 7. **(a) First beampattern DFRC carrying the target and four communications in radar active mode (the red line represents the bit "1"). The second beampattern carrying the communication (the blue dashed line represents the bit "0") (Example 2). (b) Two beampatterns with 8 sidelobe levels perform DFRC in different communication directions in radar active mode; 2nd scenario (SLL = 8).**

level associated with the higher beampattern (red line) is constrained at (−10 dB) and represents the transmitted bit "1". The communication sidelobe level associated with the lower beampattern (blue dashed line) is constrained at (−14 dB) and represents the transmitted bit "0". Note that each beampattern has one sidelobe level transmitted towards four communication users. To increase the number of sidelobe levels for the same beampattern, we propose another scenario to allow each communication user in each sidelobe to have its own power level to be transmitted towards its intended communication receiver. This can be achieved by using Eq. 5(a-c), as shown in Fig. 7(b). The first beampattern has four sidelobe levels (from left to right): $SLL_1 = -6$ dB, $SLL_2 = -7$ dB, $SLL_3 = -10$ dB and $SLL_4 = -5$ dB. Similarly, the corresponding second beampattern has the sidelobe levels: $SLL_1 = -11$ dB, $SLL_2 = -9$ dB $SLL_3 = -8$ dB and $SLL_4 = -12$ dB. Note that the behavior of these independent sidelobe levels in different communication directions enables multiuser access. In both scenarios, we consider the case of a narrow beam, and we find that the radar operation in the mainlobe is not affected by the secondary function (communication in this scenario). The SLL differences are clearly separated from each other, which definitely leads to better detection at the communication receiver ends.

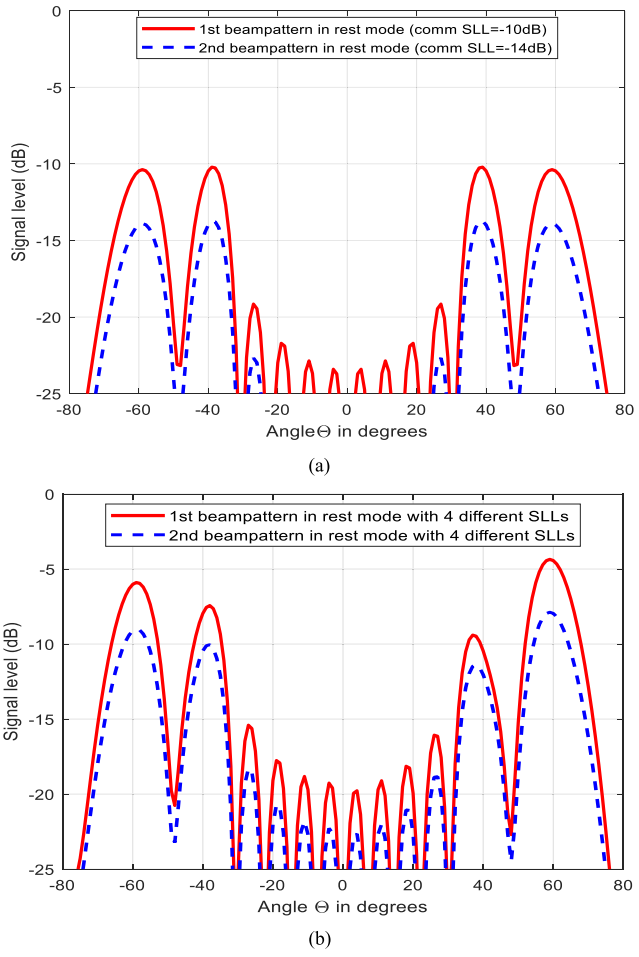

FIGURE 8. **(a) Communication transmission via GSC_2-GSC_1 producing the same SLLs (example 3); 1st scenario (SLL = 2). (b) Communication transmission via GSC2-GSC1 SLLs producing different SLLs (example 3); 2nd scenario (SLL = 8).**

Example 3 (Communication Transmission in Radar Rest Mode): With the same setup in example 2, the radar function is out of active mode, so the main beam radiation at angle $\theta_t = 0°$ towards the target goes to the deep null after every pulse width transmission. As a result, the mainlobe will not function in rest mode, while the four communication signals in the sidelobe region will keep the four communication transmission processes towards their intended receivers located at $\theta_{c1} = -60°$, $\theta_{c2} = -40°$,$\theta_{c3} = 40°$ and $\theta_{c4} = 60°$. We consider two beampatterns: each radiated beam represents either "1" or "0" using the same information embedding scheme as explained in example 2. The sidelobe levels associated with the beam patterns are constrained at SLL = −10 dB and SLL = −14 dB, as shown in Fig. 8(a). Similar to Fig. 7(b), the proposed scenario maintains the transmission

in radar rest mode to allow each communication user in each sidelobe to have its own power level to be transmitted towards its intended communication receiver, as shown in Fig. 8(b). The first beampattern has four sidelobe levels (from left to right): $SLL_1 = -6$ dB, $SLL_2 = -7$ dB $SLL_3 = -10$ dB and $SLL_4 = -5$ dB. Similarly, the corresponding second beampattern has the sidelobe levels: $SLL_1 = -11$ dB, $SLL_2 = -9$ dB, $SLL_3 = -8$ dB and $SLL_4 = -12$ dB. This mechanism/approach of using rest mode for the transmission allows the communication transmission to continue and exploit the full time of the PRI. This leads to a higher throughput and enhances the signal-to-noise ratio, as explained in this paper.

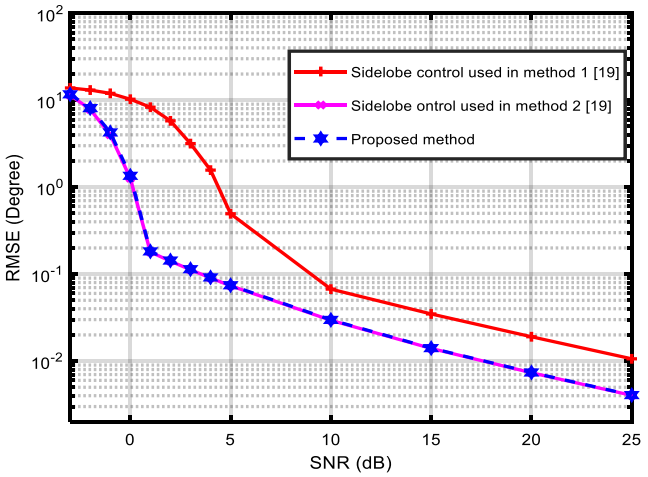

FIGURE 9. RMSEs of the DOA estimation vs the SNR.

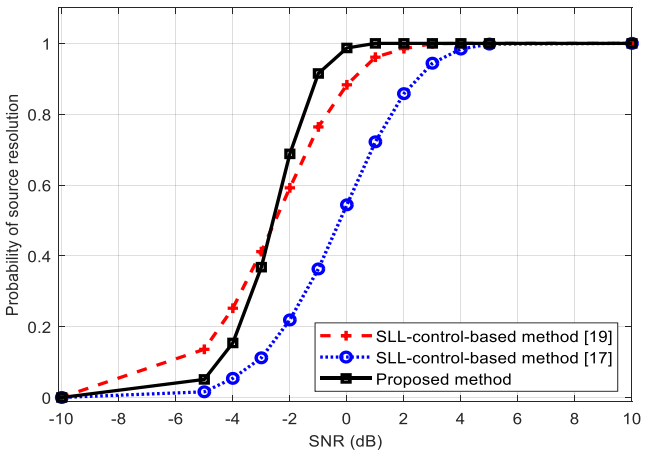

FIGURE 10. Probability of the resolution as a function of the SNR.

Example 4 (Radar Performance of the Main Beam):

Suppose that two targets are closely located 3° and 5°. We assume that the coefficients in every radar pulse are fixed. These coefficients differ from pulse to pulse. We note that the radar performance for the proposed method of dual-function radar communications outperforms the schemes [17] and [19] in terms of the root mean square error shown in Fig. 9 and the probability of resolution shown in Fig 10. The method in [17] used a single waveform in every pulse, while [19] used two waveforms, one associated with the high sidelobe beampattern and the other associated with the lower sidelobe. In our proposed method, we use two orthogonal waveforms that are transmitted with every radar pulse, which leads to better performance in terms of the direction of arrival (DOA) compared to the existing methods, to show that the system performance is identical to the result investigated in [19]. It is worth mentioning that when we increase the number of waveforms, we obtain a better result.

Example 5 (Bit Error Rate for throughput analysis):

In this example, we transmit two beamforming and compare their bit error rate with that of the existing techniques in [17] and [19]. The performance of the information embedding is computed 10^5 times. The radar mainlobe is at 0°. We transmit 2 bits in each communication beampattern to each communication receiver. The total number of bits transmitted is 8 bits for the four communication users. We design two weight vectors with two sidelobe levels varying from -10 dB for a higher sidelobe level to -14 for a low sidelobe level towards the intended communication users. For the case of multiwaveform ASK [19], the throughput in active mode is ($2\ \log_2 L$). In our case, the throughput in active mode is the same, plus the throughput in radar rest mode. The total throughput will then be written as $2\ \log_2 L + 2\ \log_2 L = 4\ \log_2 L$. Similarly, if we use any DRFC existing technique, our proposed will double the achievable throughput rate by using the same resources. We produce a higher throughput by utilizing radar rest mode as the temporal transmission domain for the sidelobe continuation transmission as calculated in section IV. We compare our results with the existing method in [17] and [19] and find that our proposed method outperforms these methods, as shown in Fig. 11.

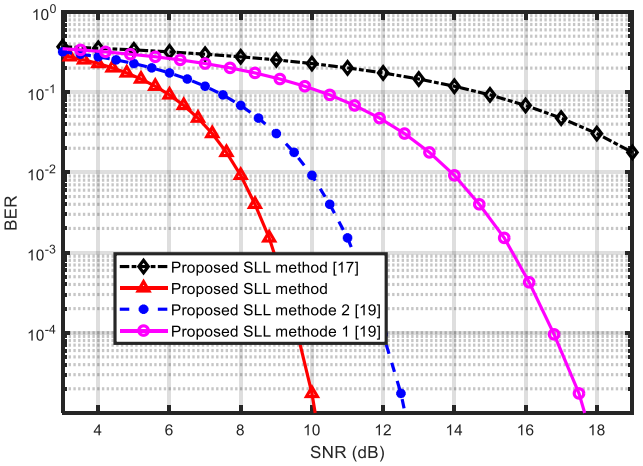

FIGURE 11. The BERs versus the SNR for four methods.

VI. CONCLUSION

In our work, we exploit the spatial and temporal resources available on the radar transmitter side to achieve a dual-function radar and communication system. We propose a technique to combine the spatial and temporal approaches

as two operational modes. One mode is the active mode, in which the radar and communication operate simultaneously. Radar is implemented via the mainlobe, and communication is implemented via the sidelobe region, followed by the second mode, known as the rest mode, in which only the communication occurs. The information embedding is obtained by changing the sidelobe levels towards multiple communication directions. We calculate the increased throughput of the communication transmission in radar rest mode. Our future work will focus on designing a robust receiver for this technique. It is worth noting that our proposed system has considerable performance in increasing the throughput and leads to a better signal-to-noise ratio while keeping the radar transmission intact. The future direction of this work will also focus on exploiting the proposed techniques with different digital modulation schemes for further investigations and enhancement.

REFERENCES

[1] C. Baylis, M. Fellows, L. Cohen, and R. J. Marks, II, "Solving the spectrum crisis: Intelligent, reconfigurable microwave transmitter amplifiers for cognitive radar," *IEEE Microw. Mag.*, vol. 15, no. 5, pp. 94–107, Jul./Aug. 2014.

[2] H. Griffiths, S. Blunt, L. Cohen, and L. Savy, "Challenge problems in spectrum engineering and waveform diversity," in *Proc. IEEE Radar Conf. (RADAR)*, Apr./May 2013, pp. 1–5.

[3] H. T. Hayvaci and B. Tavli, "Spectrum sharing in radar and wireless communication systems: A review," in *Proc. Int. Conf. Electromagn. Adv. Appl. (ICEAA)*, no. 43, Aug. 2014, pp. 810–813.

[4] H. Griffiths, L. Cohen, S. Watts, E. Mokole, C. Baker, M. Wicks, and S. Blunt, "Radar spectrum engineering and management: Technical and regulatory issues," *Proc. IEEE*, vol. 103, no. 1, pp. 85–102, Jan. 2015.

[5] C. Sahin, J. G. Metcalf, and S. D. Blunt, "Characterization of range sidelobe modulation arising from radar-embedded communications," in *Proc. Int. Conf. Radar Syst.*, Oct. 2017, pp. 1–6.

[6] A. Hassanien, M. G. Amin, Y. D. Zhang, and F. Ahmad, "Signaling strategies for dual-function radar communications: An overview," *IEEE Aerosp. Electron. Syst. Mag.*, vol. 31, no. 10, pp. 36–45, Oct. 2016.

[7] S. D. Blunt and E. L. Mokole, "Overview of radar waveform diversity," *IEEE Aerosp. Electron. Syst. Mag.*, vol. 31, no. 11, pp. 2–42, Nov. 2016.

[8] A. R. Chiriyath, B. Paul, and D. W. Bliss, "Radar-communications convergence: Coexistence, cooperation, and co-design," *IEEE Trans. Cogn. Commun. Netw.*, vol. 3, no. 1, pp. 1–12, Mar. 2017.

[9] D. W. Bliss, "Cooperative radar and communications signaling: The estimation and information theory odd couple," in *Proc. IEEE Radar Conf.*, May 2014, pp. 50–55.

[10] F. Liu, C. Masouros, A. Li, T. Ratnarajah, and J. Zhou, "MIMO radar and cellular coexistence: A power-efficient approach enabled by interference exploitation," *IEEE Trans. Signal Process.*, vol. 66, no. 14, pp. 3681–3695, Jul. 2018.

[11] M. J. Nowak, Z. Zhang, Y. Qu, D. A. Dessources, M. Wicks, and Z. Wu, "Co-designed radar-communication using linear frequency modulation waveform," in *Proc. IEEE Mil. Commun. Conf. (MILCOM)*, Nov. 2016, pp. 918–923.

[12] F. Liu, C. Masouros, A. Li, H. Sun, and L. Hanzo, "MU-MIMO communications with MIMO radar: From co-existence to joint transmission," *IEEE Trans. Wireless Commun.*, vol. 17, no. 4, pp. 2755–2770, Apr. 2018.

[13] B. Li, A. P. Petropulu, and W. Trappe, "Optimum co-design for spectrum sharing between matrix completion based MIMO radars and a MIMO communication system," *IEEE Trans. Signal Process.*, vol. 64, no. 17, pp. 4562–4575, Sep. 2016.

[14] S. D. Blunt, M. R. Cook, and J. Stiles, "Embedding information into radar emissions via waveform implementation," in *Proc. Int. Waveform Diversity Design Conf. (WDD)*, Aug. 2010, pp. 195–199.

[15] C. Sahin, J. Jakabosky, P. M. McCormick, J. G. Metcalf, and S. D. Blunt, "A novel approach for embedding communication symbols into physical radar waveforms," in *Proc. IEEE Radar Conf. (RadarConf)*, May 2017, pp. 1498–1503.

[16] S. D. Blunt, P. Yatham, and J. Stiles, "Intrapulse radar-embedded communications," *IEEE Trans. Aerosp. Electron. Syst.*, vol. 46, no. 3, pp. 1185–1200, Jul. 2010.

[17] J. Euzière, R. Guinvarc'h, M. Lesturgie, B. Uguen, and R. Gillard, "Dual function radar communication Time-modulated array," in *Proc. Int. Radar Conf.*, Oct. 2014, pp. 1–4.

[18] A. Ahmed, Y. D. Zhang, and B. Himed, "Multi-user dual-function radar-communications exploiting sidelobe control and waveform diversity," in *Proc. IEEE Radar Conf. (RadarConf)*, Oklahoma City, OK, USA, Apr. 2018, pp. 698–702.

[19] A. Hassanien, M. G. Amin, Y. D. Zhang, and F. Ahmad, "Dual-function radar-communications: Information embedding using sidelobe control and waveform diversity," *IEEE Trans. Signal Process.*, vol. 64, no. 8, pp. 2168–2181, Apr. 2016.

[20] A. Hassanien, M. G. Amin, and Y. D. Zhang, "Computationally efficient beampattern synthesis for dual-function radar-communications," *Proc. SPIE*, vol. 9829, May 2016, Art. no. 98290L.

[21] A. de Oliveira Ferreira, R. Sampaio-Neto, and J. M. Fortes, "Robust sidelobe amplitude and phase modulation for dual-function radar-communications," *Trans. Emerg. Telecommun. Technol.*, vol. 29, no. 9, p. e3314, 2018.

[22] A. De Oliveira, R. Sampaio, and J. M. Fortes, "Low-complexity robust radar-embedded sidelobe level modulation using linear constrained optimization design," in *Proc. IEEE Sensor Array Multichannel Signal Process. Workshop*, Jul. 2016, pp. 1–5.

[23] A. de Oliveira, R. Sampaio-Neto, and J. M. Fortes, "Robust radar-embedded sidelobe level modulation using constrained optimization design," in *Proc. IEEE Radar Conf.*, vol. 1, May 2016, pp. 1–5.

[24] S. Y. Nusenu, S. Huaizong, P. Ye, W. Xuehan, and A. Basit, "Dual-function radar-communication system design via sidelobe manipulation based on FDA butler matrix," *IEEE Antennas Wireless Propag. Lett.*, vol. 18, no. 3, pp. 452–456, Mar. 2019.

[25] S. Y. Nusenu, W.-Q. Wang, and A. Basit, "Time-modulated FD-MIMO array for integrated radar and communication systems," *IEEE Antennas Wireless Propag. Lett.*, vol. 17, no. 6, pp. 1015–1019, Jun. 2018.

[26] B. Paul, A. R. Chiriyath, and D. W. Bliss, "Survey of RF communications and sensing convergence research," *IEEE Access*, vol. 5, pp. 252–270, 2017.

[27] Z. U. Khan, A. N. Malik, I. M. Qureshi, and F. Zaman, "Robust generalized sidelobe canceller for direction of arrival mismatch," *Arch. Des Sci.*, vol. 65, no. 11, pp. 483–497, 2012.

[28] S. Haykin, *Adaptive Filter Theory*, 3rd ed. Upper Saddle River, NJ, USA: Prentice-Hall, 2002.

[29] A. Ahmed, Y. Gu, D. Silage, and Y. D. Zhang, "Power-efficient multi-user dual-function radar-communications," in *Proc. IEEE 19th Int. Workshop Signal Process. Adv. Wireless Commun. (SPAWC)*, Kalamata, Greece, Jun. 2018, pp. 1–5.

[30] A. Hassanien, M. G. Amin, Y. D. Zhang, and F. Ahmad, "Efficient sidelobe ASK based dual-function radar-communications," *Proc. SPIE*, vol. 9829, May 2016, Art. no. 98290K.

[31] A. Ahmed, Y. D. Zhang, and Y. Gu, "Dual-function radar-communications using QAM-based sidelobe modulation," *Digit. Signal Process.*, vol. 82, pp. 166–174, Nov. 2018.